DREXEL INSTITUTE OF TECHNOLOGY

PHILADELPHIA 4, PENNSYLVANIA

A PARAMETRIC STUDY OF THE HYPERVELOCITY PERFORATION OF VISCO-PLASTIC PLATES

PEI CHI CHOU

RICHARD W. MORTIMER

RICHARD E. LLORENS

JANUARY, 1963

DIT Report No. 125-3

DIT Report No. 125-3

DREXEL INSTITUTE OF TECHNOLOGY

PHILADELPHIA 4, PA.

A Parametric Study of the Hypervelocity Perforation of Visco-plastic Plates

PEI CHI CHOU

RICHARD W. MORTIMER

RICHARD E. LLORENS

Prepared for - Ballistic Research Laboratories
Aberdeen Proving Ground

CONTRACT NO. DA-36-034-ORD-3672 RD

January, 1963

A Parametric Study of the Hypervelocity Perforation of Visco-plastic Plates

TABLE OF CONTENTS

ABSTRACT

This report presents additional theoretical results based on a visco-plastic flow model for hypervelocity perforation of thin plates, which was given in References 1 and 2. The solutions of the governing equations including the yield strength are obtained. The results of a parametric study performed on an IBM 1620 computer are also included. The effects on the radius of perforation due to various physical quantities are discussed. The theoretical radius of perforation and residual velocity are compared with the experimental values obtained by R. W. Watson.

I. INTRODUCTION

In references 1 and 2, a visco-plastic flow theory has been presented for the solution of the hypervelocity perforation of thin plates. In this approach, the material is assumed to behave like an incompressible visco-plastic material. The perforation process is described by a simple shear plugging model. The only non-vanishing strain component is the shear strain, which is assumed constant across the thickness of the plate. The resulting equation of motion is of the diffusion type and is solved by the Laplace transform methods. The diameter of the perforated hole in the plate is then predicted by a separation criterion. For simplicity, the yield stress k was dropped from the equation.

In the present report, the solutions of the basic equations, including the yield strength, have been obtained and expressed in infinite series forms. A parametric study is then presented, in which several numerical values are assigned to each physical parameter and their effects on the radius of perforation determined.

II. BASIC EQUATIONS

Under the assumption of the simplified perforation model, the only equation of motion is

$$\frac{\partial \tau}{\partial r} + \frac{\tau}{r} = \rho \frac{\partial^2 z}{\partial t^2} \tag{1}$$

The visco-plastic property of the material is assumed to be

$$\tau = \mu \frac{\partial \gamma}{\partial t} - k \tag{2}$$

The relations between the strain , axial displacement and the velocity are

$$\begin{aligned} \gamma &= \frac{\partial z}{\partial r} \\ v &= \frac{\partial z}{\partial t} \\ \frac{\partial \gamma}{\partial t} &= \frac{\partial v}{\partial r} \end{aligned} \tag{3}$$

Combining Equations 1, 2 and 3 yields the following governing differential equation,

$$\frac{\partial^2 v}{\partial r^2} + \frac{1}{r}\frac{\partial v}{\partial r} - \frac{1}{r}\frac{k}{\mu} = \frac{1}{\nu}\frac{\partial v}{\partial t}$$

The initial and boundary conditions may be expressed as

$$v = 0 \qquad \text{AT} \quad t = 0,\ r > a$$

$$v = v_o \qquad \text{AT} \quad t = 0^+,\ r = a$$

$$h'\mu \frac{\partial v}{\partial r} - h'k - \frac{\partial v}{\partial t} = 0 \qquad \text{AT} \quad t > 0,\ r = a$$

$$v \to 0 \qquad \text{AT} \quad r \to \infty$$

where $h' = \frac{2\pi a h}{M}$

Equations 4 and 5 may be made dimensionless by introducing the Reynold's number and Bingham's number,

$$R = \text{Reynold's Number} = \frac{v_o \rho a}{\mu}$$

$$B = \text{Bingham's Number} = \frac{ak}{\mu v_o}$$

and the dimensionless quantities: r', t' and v' defined by

$$r' = \frac{r}{a} \quad ; \qquad t' = \frac{t v_o}{a} \quad ; \qquad v' = \frac{v}{v_o}$$

The resulting equations are

$$\frac{\partial^2 v'}{\partial r'^2} + \frac{1}{r'}\frac{\partial v'}{\partial r'} - \frac{1}{r'}B = R\frac{\partial v'}{\partial t'} \qquad \text{AT} \quad t' > 0,\ r' > 1$$

$$v' = 0 \qquad \text{AT} \quad t' = 0,\ r' > 1$$

$$v' = 1 \qquad \text{AT} \quad t' = 0,\ r' = 1$$

$$\frac{\partial v'}{\partial r'} - B - R\frac{\partial v'}{\partial t'} = 0 \qquad \text{AT} \quad t' > 0,\ r' = 1$$

$$v' = 0 \qquad \text{AT} \quad t' \geq 0,\ r' = \infty$$

where $H = \frac{2\pi a^2 h \rho}{M}$ is a dimensionless mass ratio.

Equations 6 to 10, with $B=0$, have previously been solved and the results reported in Reference 2. In this report, solutions are obtained for the case $B \neq 0$ by using Laplace transform and asymptotic expansion techniques. The results, which are summarized in Appendix I, are in the

form of equations for v'., z' , $\frac{\partial z'}{\partial r'}$ and $\frac{\partial v'}{\partial r'}$ in terms of t' and r' For any given set of values of parameters R, B and H, these dimensionless quantities may be calculated from Equations I-14, I-15, I-16 and I-17, respectively. The calculations involved have been programmed on an IBM 1620 computer. The output from the computer is either in tabular form or in graph form, plotted as $\frac{\partial z'}{\partial r'}$ vs. r' and $\frac{\partial v'}{\partial r'}$ vs. r' curves at different time intervals. A typical set of curves, plotted by the computer, are shown in Figures 1 and 2.

The same separation criterion as presented in Reference 2 is used here for the prediction of the perforation diameter. This criterion stipulates that separation occurs when the plate material changes from a "viscous fluid" to a "non-viscous" fluid. It is further assumed that the material is viscous when the viscous stress is larger than the yield stress; the material is considered a fluid only if the strain is larger than a constant, in this case the static ultimate shear strain is used. In equation form, this separation criterion states that separation occurs when

$$\mu \frac{\partial v}{\partial r} \leq \tau_0 \quad \text{AND} \quad \frac{\partial z}{\partial r} \geq \gamma_0 \tag{11}$$

The actual procedure in applying this criterion and in finding the radius of perforation is shown in Figures 1, 2 and 3. In Figure 1, a horizontal dotted line is drawn for a particular value of γ_0 From the intersections between this line and the strain vs. radius curves, the critical strain curve may be constructed as shown in Figure 3. Similarly, the critical strain-rate curve may be constructed from Figure 2. The intersection between the critical strain and critical strain-rate curves gives the radius of perforation r_p and the time t_p when separation occurs.

III. PARAMETRIC STUDY

A parametric study was performed in order to find out the effect on the perforation process due to different parameters. The parameters used were dimensional physical quantities, such as plate thickness (inch) and projectile velocity (ft/sec), rather than dimensionless quantities B, R, and H. This approach was used to obtain directly the effect due to physical quantities. The following parameters were studied: projectile velocity V_o, projectile diameter a, projectile mass M_1, plate thickness h, plate density ρ, yield strength k, coefficient of viscosity μ, ultimate shear strength τ_o and ultimate shear strain γ_o. A set of base values for these parameters was first chosen, the strain and strain-rate distributions were calculated and the radius of perforation determined. Then, each parameter was varied individually with all the other parameters held at their base values. The effect on the radius of perforation due to each parameter was evaluated and discussed.

The set of base values used are

V_o = 3170. m/sec

a = 1/32"

h = 1/16", 1/8", 3/16", 1/4"

M_1 = .025 gm

μ = 100 lb-sec/ft^2

k = 24,000 psi

ρ = 5.3707963 slug/ft^3

τ_o = 91,000 psi

γ_o = .02

The values for V_o, a, h and M_1, are similar to those used in a series of experiments performed by Watson, as shown in Reference 3. The values for the rest of the parameters, all pertaining to material properties, were either taken from handbooks or estimated. A coefficient of viscosity of 100 lbs-sec/ft^2 is believed to be a reasonable estimated value as

discussed in Reference 1. The yield strength in shear of the plate and the density of the plate are those properties of 2024-T3 aluminum. An ultimate strength of the plate of 91,000 psi was assumed for dynamic conditions. Finally, the critical strain of .02 was used because the ultimate strain of 2024-T3 aluminum under static conditions is of the order of magnitude of one per cent.

IV. RESULTS AND DISCUSSIONS

The numerical values used for the parameters, together with the calculated results, are presented in Table 1. These results are also plotted in curves as shown in Figures 4 to 10. In these figures, the radius of perforation r'_p is plotted as ordinate and the plate thickness h as abscissa, with one particular physical quantity as parameter. Three curves are shown on each figure representing three values of the parameter under consideration, one at the base value, one above and one below. These curves are discussed in the following paragraphs. In addition, the combined effect of the ultimate strength and ultimate strain are discussed in Section 10. Comparisons with test data are given in Sections 11 and 12.

1. Plate Thickness

In Figures 4 to 10, it can be seen that an increase in plate thickness decreases the r'_p, regardless of the other parameters involved.

2. Plate Density

Figure 4 shows the effect of the variation of the plate density on the dimensionless perforation radius. By increasing the density

from 5.37 slug/ft^3 to 10.74 slug/ft^3 the r'_p is decreased throughout the four thicknesses. A decrease in the density to 2.685 slug/ft^3 increases r'_p over all plate thicknesses. This range of density includes such materials as aluminum, beryllium and magnesium.

3. Coefficent of Viscosity

The effect on r'_p due to the variations of the coefficent of viscosity is shown in Figure 5. A decrease in r'_p is caused by a decrease in viscosity from 100 lb-sec/ft^2 to 50 lb-sec/ft^2 and an increase is observed when the viscosity was raised to 200 lb-sec/ft^2. This range was found to be sufficient to evalutate the trend. The larger value of viscosity is seen to have a considerable effect on the r'_p.

4. Projectile Velocity

Figure 6 shows that an increase of the projectile's initial velocity from 10,400 fps. to 20,800 fps enlarges the r'_p while a decrease to 7800 fps decreases the r'_p. This range of velocities represents the current laboratory capability and perforation test data at this velocity range are expected to be available shortly.

5. Ultimate Strength

In Figure 7, the ultimate strength (σ_o) is decreased from 91,000 psi to 65,000 psi resulting in an increase of r'_p. With σ_o increased to 125,000 psi the r'_p is decreased. This range was used due to the uncertainity of the dynamic value of the ultimate strength.

6. Critical Strain

The critical strain (γ_o) effect on r'_p is shown in Figure 8.

The r'_p is increased for an increase of γ_o from .02 to .035. For a decreased value of γ_o of .005 the r'_p is decreased. This range of γ_o represents a reasonable variation of strain from the static ultimate strain of .01.

7. Projectile Mass

In Figure 9 the effect of the variation of projectile mass on the dimensionless perforation radius is shown. When the mass is increased from 1.71×10^{-6} slugs to 3.42×10^{-6} slugs a larger r'_p is observed. With a decrease of the mass to $.86 \times 10^{-6}$ slugs a smaller r'_p is obtained. The radius of the projectile was kept constant for these three values of the projectile mass. This change of mass may be accomplished by a change of either length or density of the projectile.

8. Projectile Radius

The variation of r_p with the change in projectile radius is shown in Figure 10. Since $r'_p = r_p/a$, it is necessary to show the dimensional r_p variation with a. An increase in the projectile's radius from .03125 inch to .0442 inch produces a slight increase in r_p. While a decrease to .0221 inch causes a small decrease in r_p. However, the differences between all three are rather small. The mass of the projectile was held constant throughout this series, therefore, this change in the projectile's radius would be accompanied by a change in either the length or density of the projectile.

9. Yield Strength

When k is decreased from 24,000 psi to 5000 psi the r'_p is unchanged. With the exception of one case (Run #39, h = 1/4"), increasing k to 48,000 psi does not change the perforation radius.

For Run #39, the r'_p is slightly increased. This range of yield strength values was used to account for the possible variation due to the dynamic effect.

10. Combined Effect of δ_o and V_o

In Figure 11 it can be seen that a particular diameter can be obtained from the critical strain and strain-rate curves by varying either the critical strain and/or ultimate strength of the plate material.

a) Critical Strain Constant

An increase in ultimate strength from 91,000 psi to 125,000 psi will decrease both the r'_p and t'_p. Decreasing the ultimate strength to 65,000 psi increased the r'_p and t'_p.

b) Ultimate Strength Constant

Increasing critical strain from .02 to .035 increased the r'_p and t'_p. A decrease to .005 decreased these same quantities.

c) Variation of Both Strain and Ultimate Strength

By observing Figure 11 one can see that many combinations of critical strain and ultimate strength yield a particular value for r'_p. However, the t'_p varied for each combination of critical strain and ultimate strength.

11. Residual Velocity

The residual velocity, (or the velocity of the projectile after the perforation process is completed), is calculated for a few cases. These are shown in Figure 12 in which the velocity V_o is also presented.

The velocity U_o is calculated by a simple momentum exchange between the projectile and the portion of the plate directly in contact with it. The quantity M (V_o-Vres) represents the momentum transferred to the perforated plate fragments (spall).

Comparing these curves with the test data of Reference 3, an apparent discrepancy appears. In particular, it may be observed in Figure 12, that at a plate thickness of .31 cm, the test residual velocity is much higher than the theoretical. There are two possible explanations for this discrepancy. First, the spall may flash back in a direction opposite to that of the projectile, and as a result, the forward residual momentum and velocity are increased; or, second, the portion of the plate directly in contact with the projectile may leave the plate with a velocity less than the residual velocity of the projectile. However, according to Watson's experiments, there was no flash-back observed in the perforation of aluminum plates. Presently, the Bureau of Mines is conducting tests to determine the residual velocity of the spall in order to evaluate the feasibility of the second explanation regarding this inconsistency.

12. Comparison of r'_p With Test Data

Observation of Figure 13 shows the comparison of the perforation diameter of various thicknesses of aluminum 2024-T3 plate. At a plate thickness of 1/16" there is a discrepancy with the theoretical value being slightly higher. However, for the other plate thicknesses (1/8", 3/16"), there is general agreement.

V. TABLE AND FIGURES

TABLE 1 - RESULTS OF PARAMETRIC STUDY

S	μ	Vo	M_1	A	k	∇To	δ_o	h	R	B	H	r_p'	
slug/ft^3	lb-sec/ft^2	FPS	SLUGx10^5	ft.x10^{-3}	psix10^{-4}	psix10^{-4}	in/in	in.					RUN
								1/16	1.07	.011	.516	3.60	1
* 5.37	100	10,400	.171	2.6	2.4	9.1	.02	1/8	.858	.014	.821	3.24	2
								1/4	.608	.021	1.16	2.78	3
								1/16	.619	.010	.296	4.18	4
2.68								1/8	.539	.012	.516	3.92	5
	100	10,400	.171	2.6	2.4	9.1	.02	1/4	.429	.015	.821	3.51	6
								1/16	1.71	.015	.821	3.20	7
10.7								1/8	1.22	.021	1.16	2.72	8
								1/4	.769	.033	1.47	2.28	9
								1/16	2.18	.023	.516	2.52	10
	50							1/8	1.72	.029	.821	2.38	11
5.37		10,400	.171	2.6	2.4	9.1	.02	1/4	1.22	.041	1.16	2.10	12
								1/16	.540	.006	.516	6.00	13
	200							1/8	.429	.007	.820	5.62	14
								1/4	.304	.010	1.16	5.33	15
								1/16	.809	.016	.516	3.33	16
		7800						1/8	.643	.020	.820	2.99	17
5.37	100		.171	2.6	2.4	9.1	.02	1/4	.456	.028	1.16	2.38	18
								1/16	2.16	.006	.516	4.30	19
		20,800						1/8	1.72	.007	.821	3.91	20
								1/4	1.22	.010	1.16	3.42	21
								1/16	.858	.015	.821	3.28	22
			.086					1/8	.608	.021	1.16	2.78	23
5.37	100	10,400		2.6	2.4	9.1	.02	1/4	.384	.033	1.47	2.19	24
								1/16	1.24	.010	.296	3.80	25
			.342					1/8	1.08	.012	.516	3.70	26
								1/4	.858	.015	.821	3.27	27
								1/16	.876	.007	.296	4.78	28
				1.8				1/8	.763	.008	.516	4.40	29
5.37	100	10,400	.171		2.4	9.1	.02	1/4	.607	.010	.821	3.96	30
								1/16	1.21	.021	.821	2.73	31
				3.6				1/8	.860	.030	1.16	2.42	32
								1/4	.544	.046	1.47	2.00	33
								1/16	1.07	.002	.516	3.60	34
					.50			1/8	.858	.003	.821	3.24	35
5.37	100	10,400	.171	2.6		9.1	.02	1/4	.608	.004	1.16	2.78	36
								1/16	1.07	.023	.516	3.60	37
					4.8			1/8	.858	.029	.821	3.24	38
								1/4	.608	.041	1.16	3.76	39
								1/16	1.07	.011	.516	---	40
						6.5		1/8	.858	.014	.821	3.62	41
5.37	100	10,400	.171	2.6	2.4		.02	1/4	.608	.021	1.16	3.19	42
								1/16	1.07	.011	.516	3.20	43
						12.5		1/8	.858	.014	.821	2.90	44
								1/4	.608	.021	1.16	2.48	45
								1/6	1.07	.011	.516	2.88	46
							.005	1/8	.858	.014	.821	2.72	47
5.37	100	10,400	.171	2.6	2.4	9.1		1/4	.608	.021	1.16	2.52	48
								1/16	1.07	.011	.516	---	49
							.035	1/8	.858	.014	.821	3.40	50
								1/4	.608	.021	1.16	2.88	51

*BASE VALUES

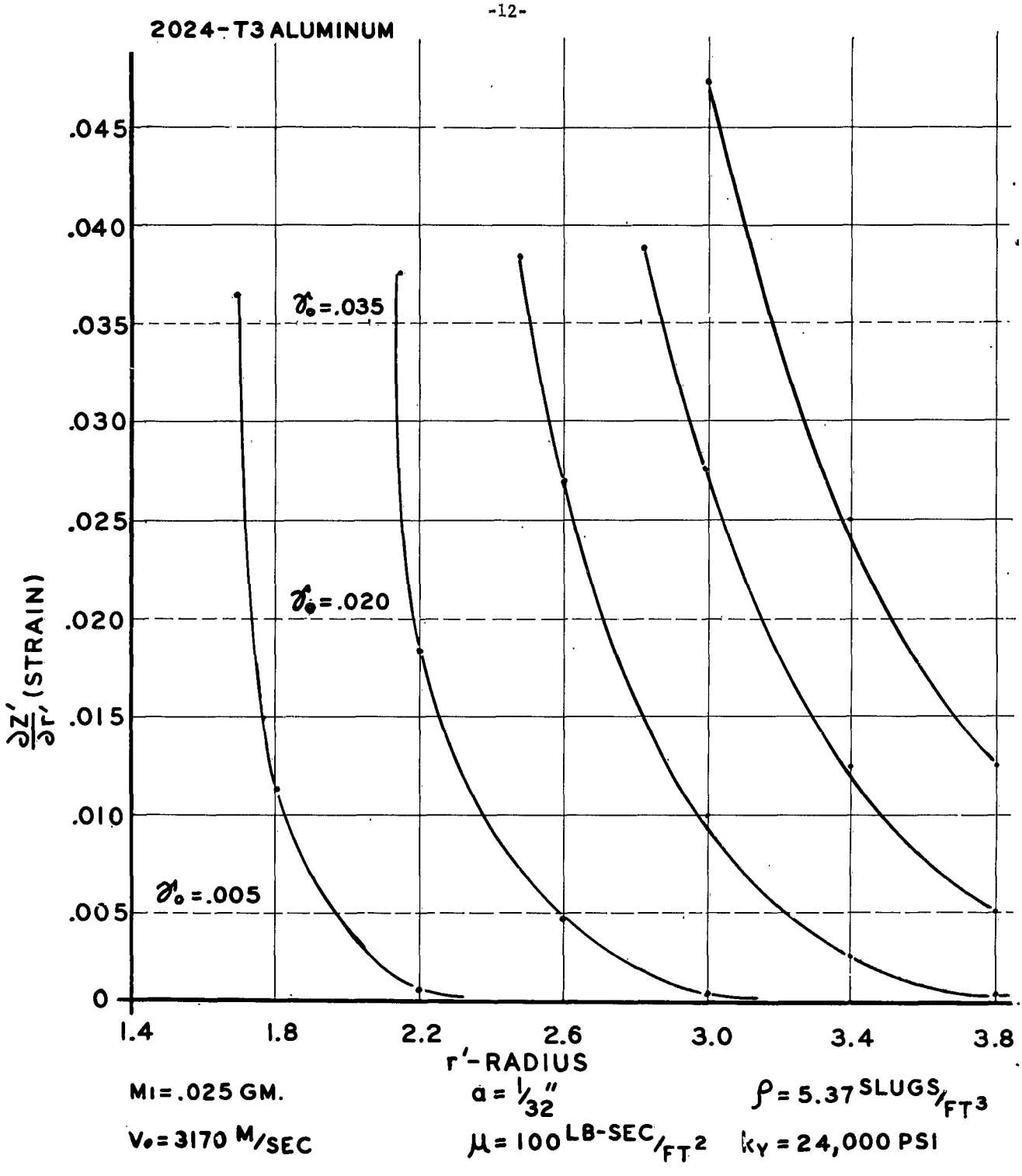

FIG. 1 STRAIN VS. RADIUS (h = 1/8")

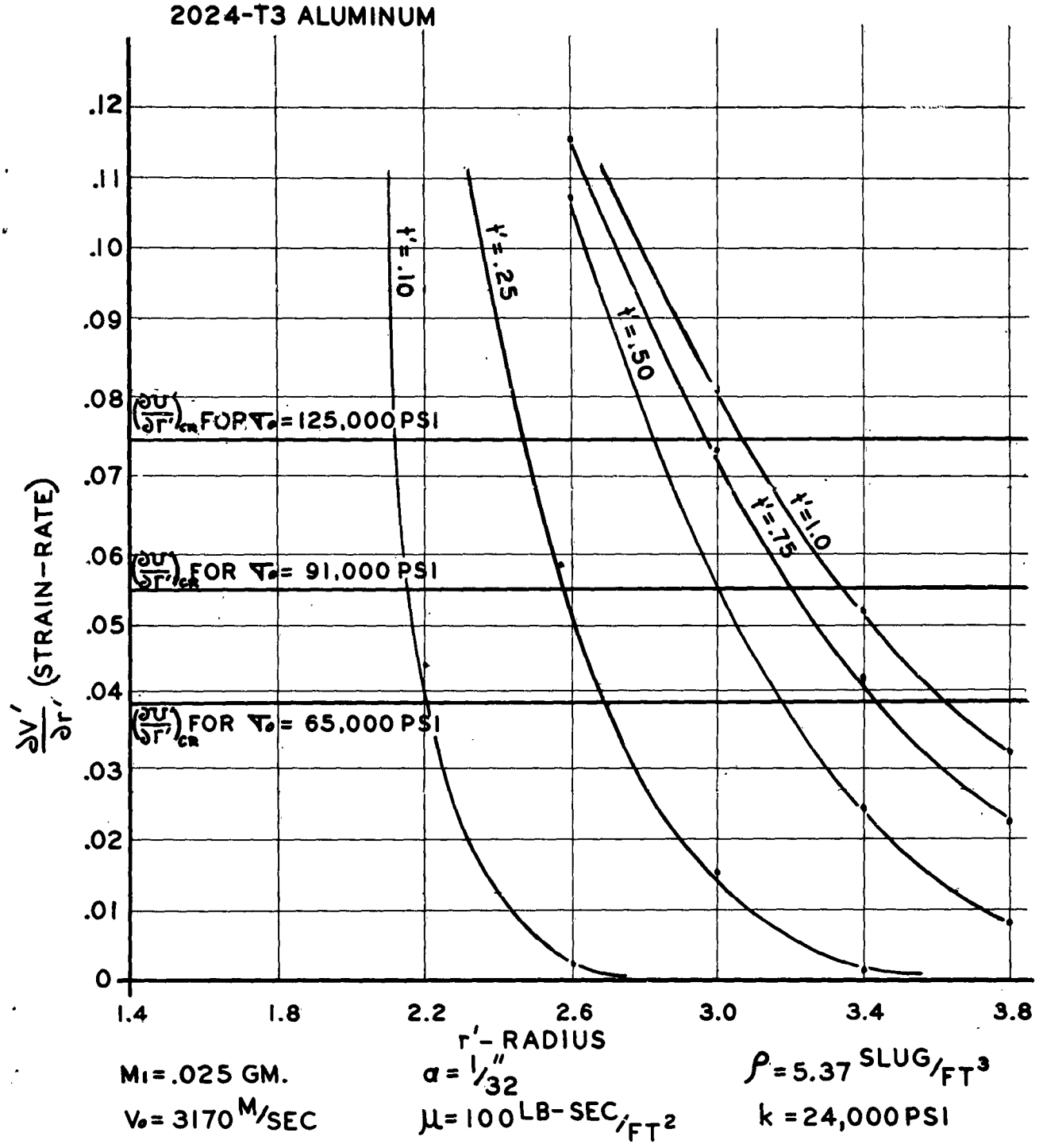

FIG. 2 STRAIN-RATE VS. RADIUS ($h = 1/8''$)

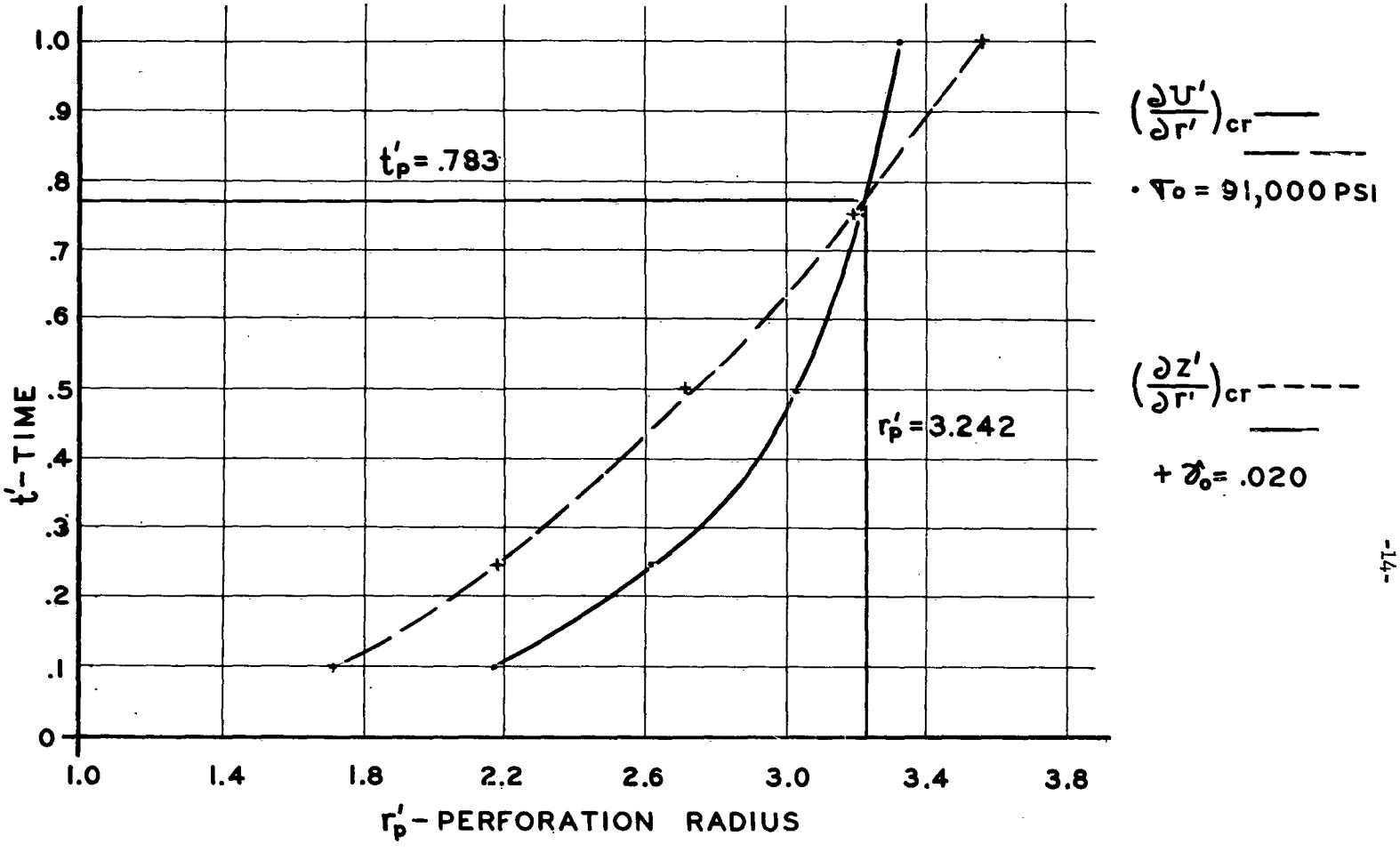

FIG. 3 CRITICAL STRAIN $\left(\frac{\partial Z'}{\partial r'}\right)_{cr}$ AND STRAIN-RATE $\left(\frac{\partial U'}{\partial r'}\right)_{cr}$ CURVES FOR BASE VALUES OF ULTIMATE STRENGTH (τ_o) AND CRITICAL STRAIN (γ_o)

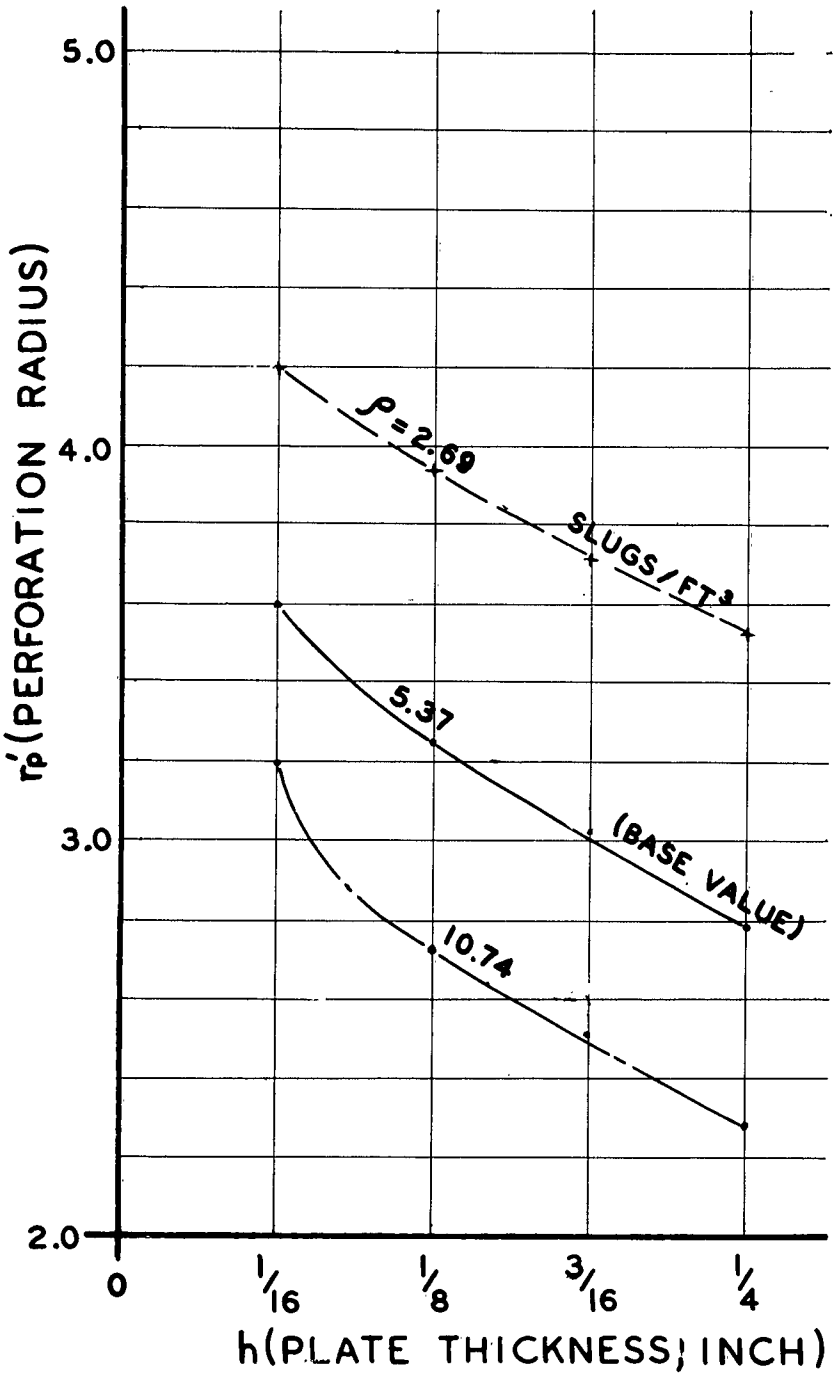

FIG. 4 THE EFFECT OF THE PLATE DENSITY (ρ) ON THE PERFORATION RADIUS

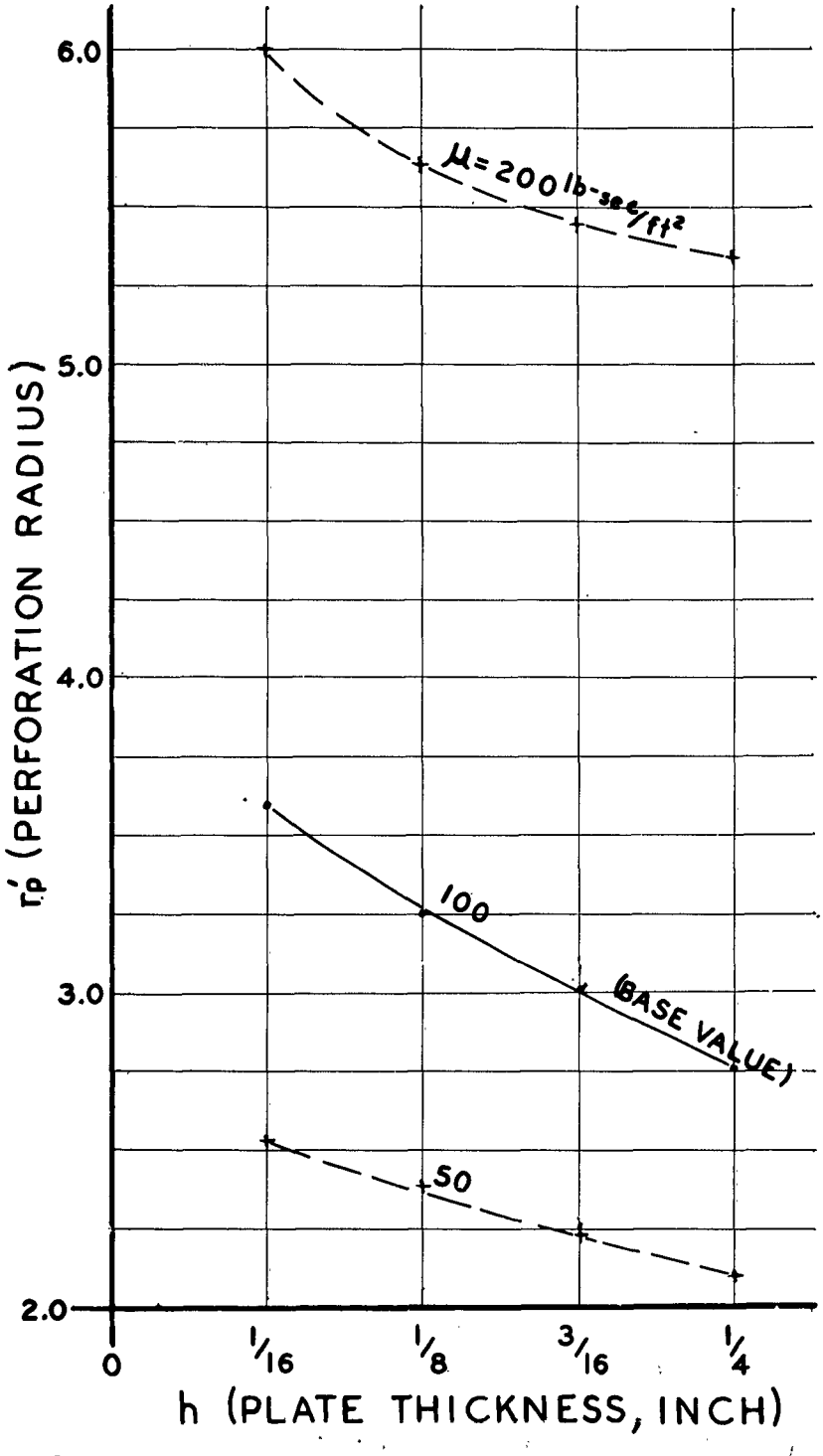

FIG. 5 THE EFFECT OF THE COEFFICIENT OF VISCOSITY (μ) ON THE PERFORATION RADIUS

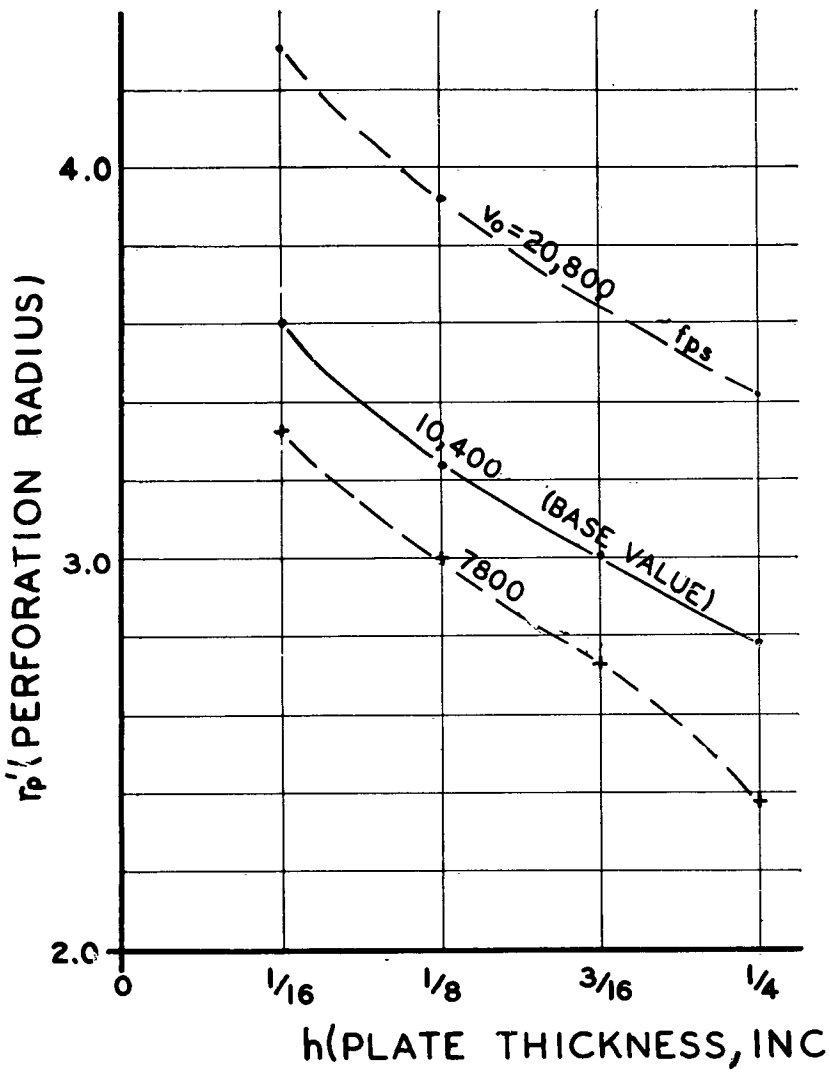

FIG. 6 THE EFFECT OF THE INITIAL PROJ. VELOCITY (V_o) ON THE PERFORATION RADIUS

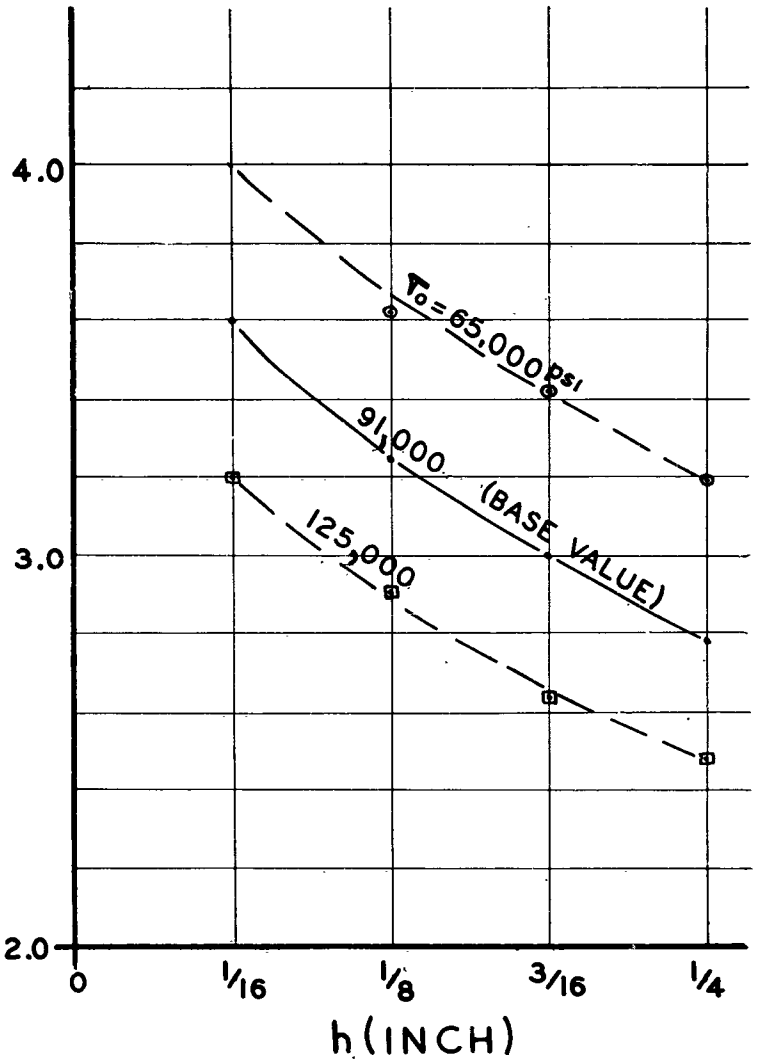

FIG. 7 THE EFFECT OF ULTIMATE STRENGTH ($\bar{\sigma}_o$) ON THE PERFORATION RADIUS

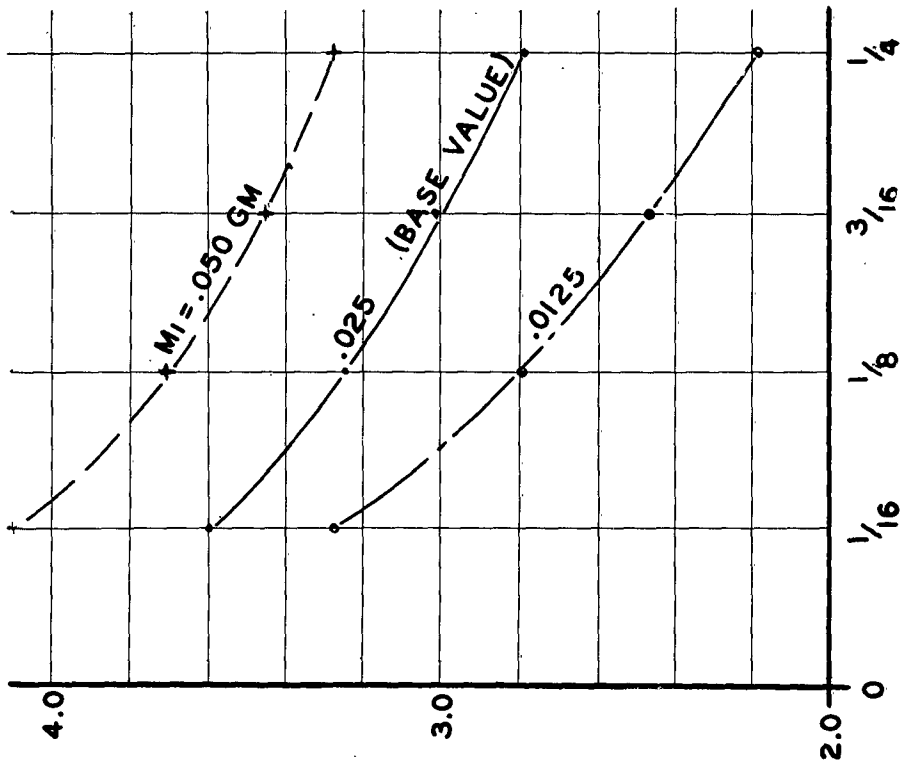

FIG. 9 THE EFFECT OF THE MASS OF PROJECTILE (M_1) ON THE PERFORATION RADIUS

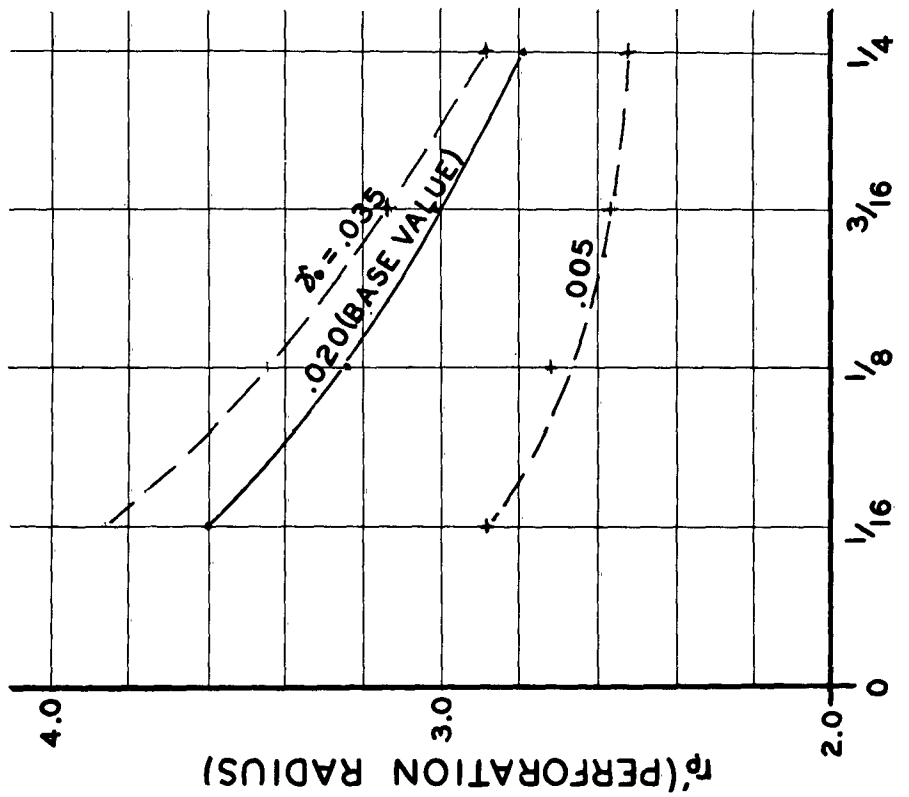

FIG. 8 THE EFFECT OF CRITICAL STRAIN (γ_0) ON THE PERFORATION RADIUS

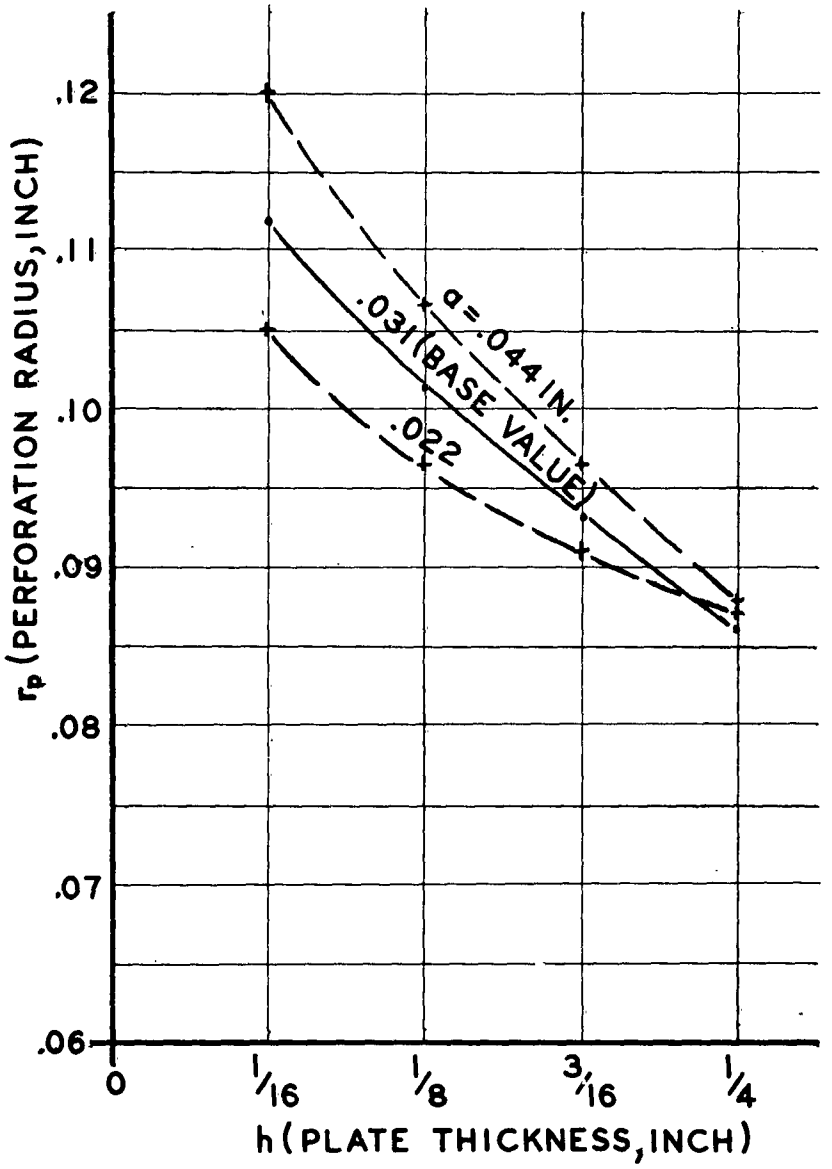

FIG.10 THE EFFECT OF THE RADIUS OF PROJECTILE(a) ON THE PERFORATION RADIUS

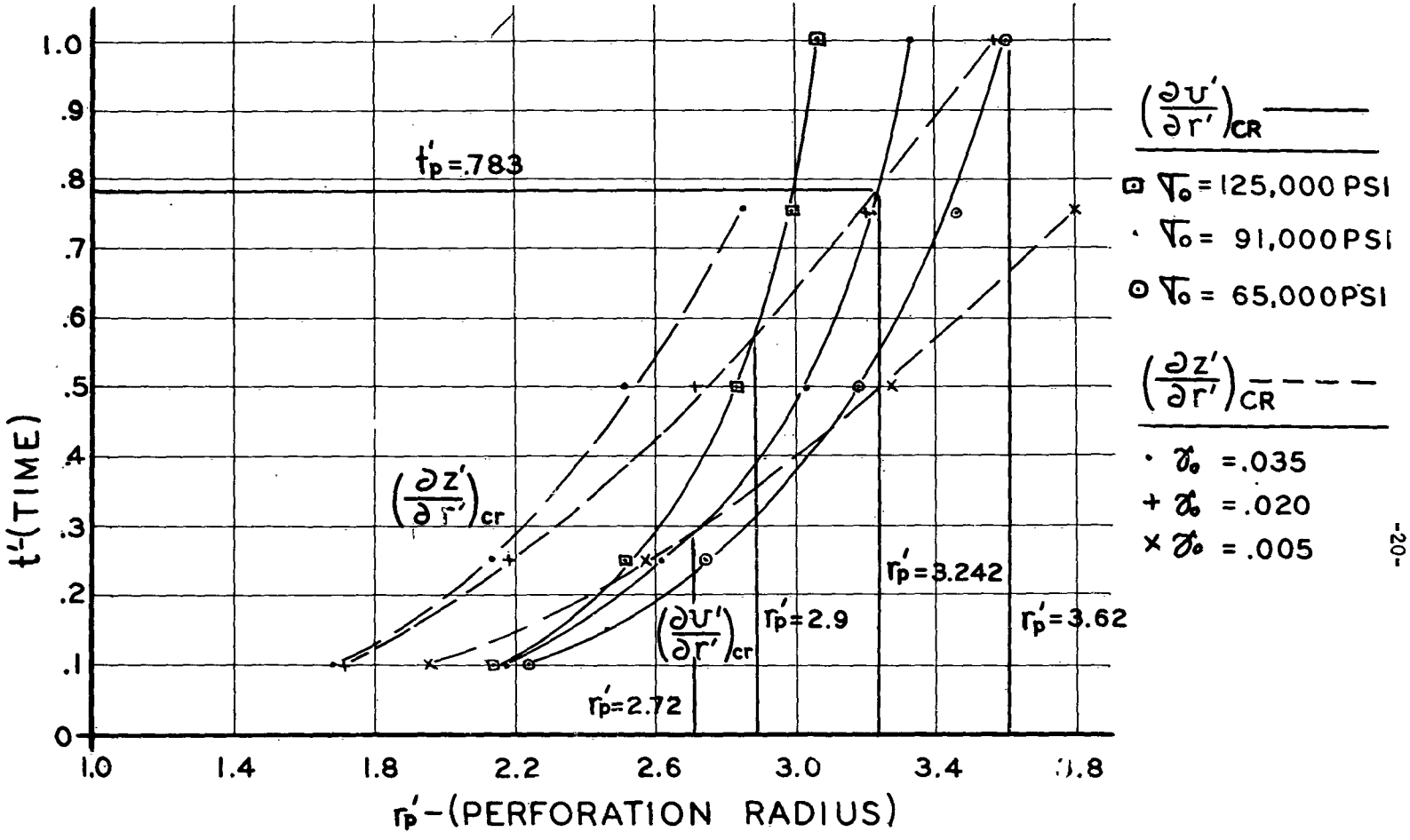

FIG.11 CRITICAL STRAIN $(\frac{\partial z'}{\partial r'})_{cr}$ AND STRAIN-RATE $(\frac{\partial u'}{\partial r'})_{cr}$ CURVES FOR VARIOUS VALUES OF ULTIMATE STRENGTH (σ_0) AND CRITICAL STRAIN (γ_0) $h = 1/8''$

$a = \frac{1}{32}$"

$M_1 = .025$ gm

$V_o = 3170$ m/sec

•— CARNEGIE TEST RESIDUAL VELOCITY

+—THEORETICAL $V_o = \frac{V_o M_1}{M_{total}}$

o— THEORETICAL RESIDUAL VELOCITY

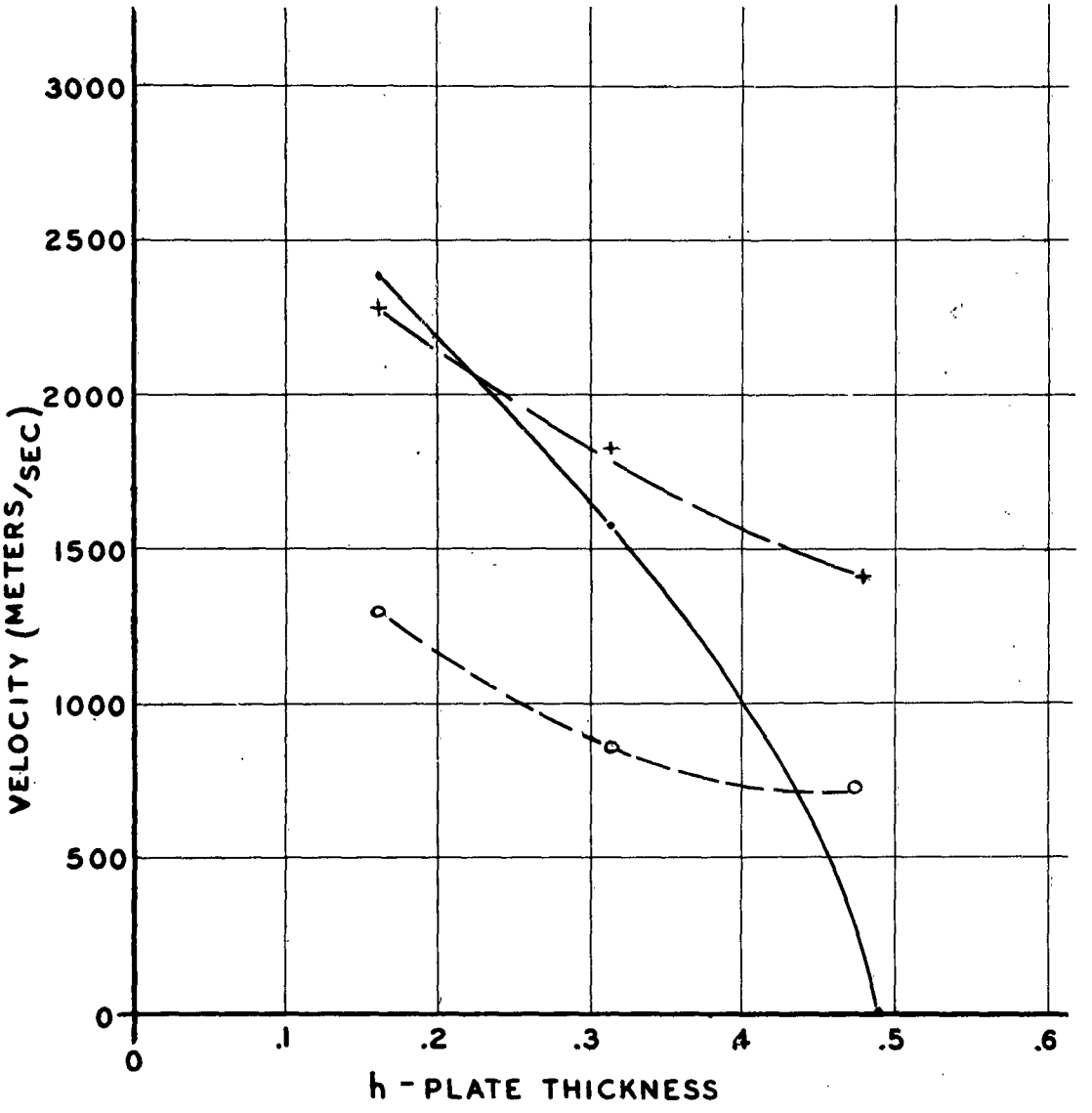

FIG. 12 RESIDUAL VELOCITY VS. PLATE THICKNESS FOR 2024-T3 ALUMINUM

ORIGINAL VELOCITY = 3170 M/SEC
RADIUS OF PROJECTILE = 1/32"
PLATE MATERIAL = 2024-T3 AL
MASS OF PROJECTILE = .025 GM.

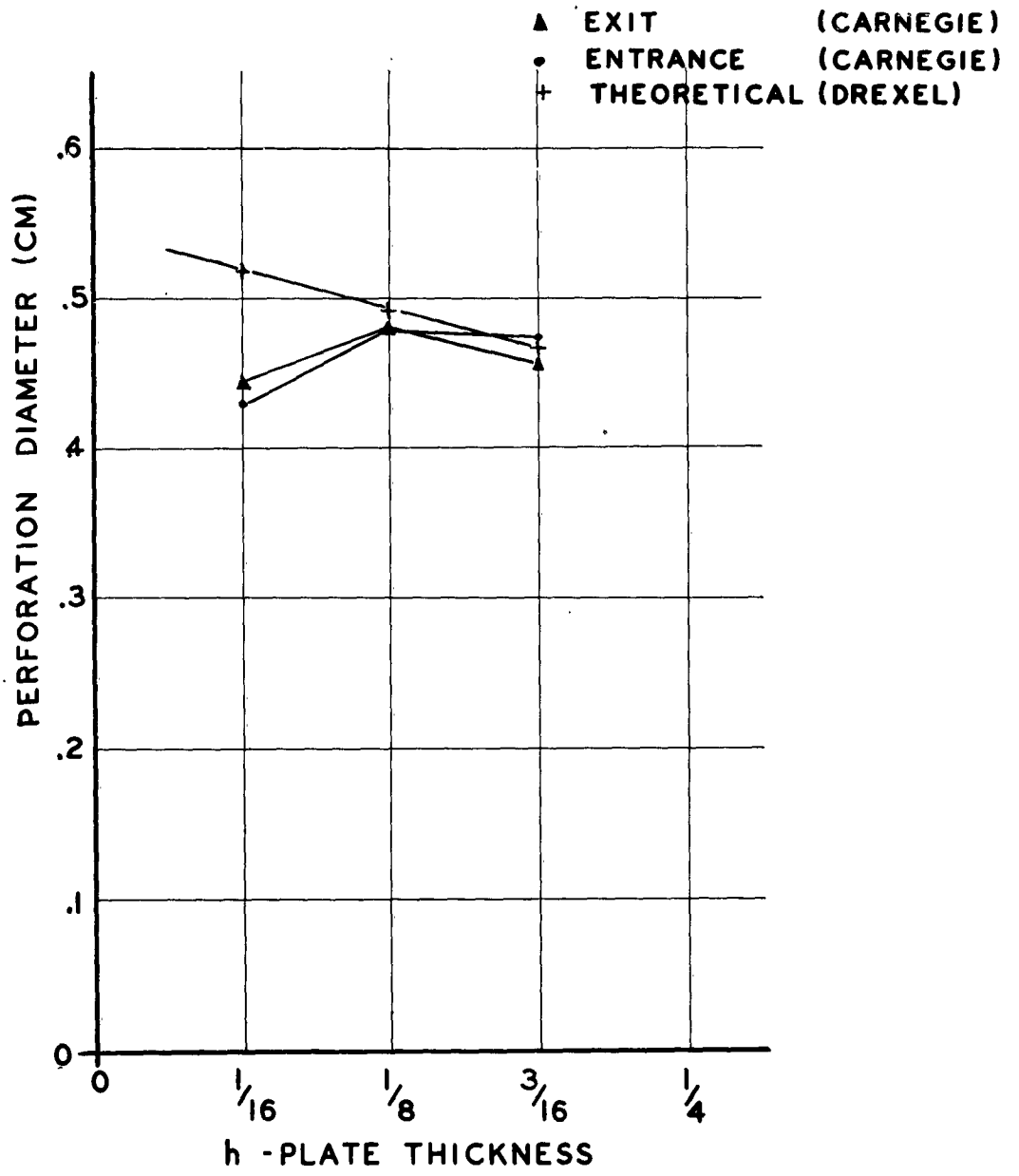

FIG. 13 COMPARISON OF PERFORATION DIAMETERS— CARNEGIE'S TEST RESULTS VS. THEORETICAL

VI. REFERENCES

1. Chou, P. C., "Perforation of Plates by High Speed Projectiles", Developments in Mechanics, Vol. I, (Proceedings of the Seventh Midwestern Mechanics Conference, Sept. 6-8, 1961, Michigan State Univ.), Plenum Press Inc., N. Y., N. Y.

2. Chou, P. C., "Visco-Plastic Flow Theory in Hypervelocity Impact", Proc. 5th Synposium on Hypervelocity Impact, Denver, Colo., Oct. 1961.

3 Watson, R. W., "The Perforation of Thin Plates by High Velocity Fragments", Proc. 5th Symposium on Hypervelocity Impact, Denver, Colo., Oct. 1961.

4. Watson, G. N., "A Treatise on the Theory of Bessel Functions", (Cambridge, 1944).

5. Carslaw, H. S., and Jaeger, J. C., "Conduction of Heat in Solids", (Oxford University Press, 1959), 2nd Edition, pp. 494-496.

VIII. NOTATIONS

a = Radius of projectile

B = Bingham No. = $\frac{ak}{\mu v_o}$

C = Constants

h = Thickness of plate

H = Mass Ratio = $\frac{2\pi a^2 h \rho}{M}$

k = Yield Strength in Shear

M = $M_1 + \pi a^2 h \rho$

M_1 = Mass of projectile

r = Radial distance

r' = Dimensionless radial distance = $\frac{r}{a}$

r'_p = Dimensionless perforation radial distance

R = Reynold's No. = $\frac{v_o \rho a}{\mu}$

t = Time

t' = Dimensionless time = $\frac{tv_o}{a}$

v = Velocity

v' = Dimensionless Velocity = $\frac{v}{v_o}$

v_o = Initial velocity

z = Displacement

z' = Dimensionless displacement

γ_o = Critical Strain

ρ = Density of plate

μ = Coefficient of Viscosity

ν = Kinematic Coefficient of Viscosity = $\frac{\mu}{\rho}$

$\frac{\partial v'}{\partial r'}$ = Dimensionless Strain - rate

$\left(\frac{\partial v'}{\partial r'}\right)_{cR}$ = Dimensionless Critical Strain - rate

$-\frac{\partial z'}{\partial r'}$ = Dimensionless Strain

VIII. APPENDIX I: Solution of the Governing Equations

Applying the Laplace transform to Equation 6 results in

$$\frac{\partial^2 \bar{v}}{\partial r'^2} + \frac{1}{r'}\frac{\partial \bar{v}}{\partial r'} - \frac{1}{r'}\frac{\bar{b}}{p} = q^2 \bar{v} \qquad \text{(I-1)}$$

where $\bar{v}$ is the transform of v', $q^2 = Rp$ and p is the parameter of the transform. Introducing

$$\bar{r} = q r' \quad , \qquad \bar{a} = q a' \quad \text{AND} \quad C = \frac{\bar{b}}{q p}$$

Equation (I-1) becomes

$$\frac{\partial^2 \bar{v}}{\partial \bar{r}^2} + \frac{1}{\bar{r}}\frac{\partial \bar{v}}{\partial \bar{r}} - \bar{v} = \frac{C}{\bar{r}} \qquad \text{(I-2)}$$

The boundary conditions, Equations 9 and 10, transform into

$$q\frac{\partial \bar{v}}{\partial \bar{r}} - \frac{\bar{b}}{p} - \frac{R}{H}\left(p\bar{v} - 1\right) = 0 \qquad \text{(I-3)}$$

$$\text{AS} \quad \bar{r} \longrightarrow \infty \ , \ \bar{v} = 0 \qquad \text{(I-4)}$$

The initial conditions are satisfied by the transforms (I-2) and (I-3). The general solution of the homogeneous equation associated with Equation (I-2) is

$$\bar{v} = A K_o(\bar{r}) + B_o I_o(\bar{r}) \qquad \text{(I-5)}$$

where I_o and K_o are the modified Bessel Functions of the zero order, and of the first and second kind respectively; A and B_o are constants. The particular solution for Equation (I-2) is obtained by the method of variation of parameters. The Wronskian of the general solution of the homogeneous equation is

$$W = (K_o I_o' - I_o K_o') = \frac{1}{\bar{r}} \qquad \text{(I-6)}$$

where the prime represents differentiation. It can be shown that the particular solution of Equation (I-2) is

$$\bar{U} = C\left[I_o \int K_o \, d\bar{r} - K_o \int I_o \, d\bar{r} \right] \tag{I-7}$$

The general solution of Equation (I-2) is thus

$$\bar{U} = AK_o(\bar{r}) + B_o I_o(\bar{r}) + C\left[I_o \int K_o \, d\bar{r} - K_o \int I_o \, d\bar{r} \right] \tag{I-8}$$

At $\bar{r} = \infty$, the functions K_o, $I_o \int K_{od} \bar{r}$ and $K_o \int I_{od} \bar{r}$ all vanish. Therefore, to satisfy Equation (I-4), it is only necessary to set $B_o = 0$. Substituting Equation (I-8) into Equation (I-3) yields the constant A,

$$A = \frac{1 - \frac{HB}{pR} + \int_{\bar{a}} K_o \, d\bar{r}\, C\left[\frac{H}{R} q I_o'(\bar{a}) - pI_o(\bar{a})\right] + \int_{\bar{a}} I_o \, d\bar{r}\, C\left[-\frac{H}{R} q K_o'(\bar{a}) + pK_o(\bar{a})\right]}{pK_o(\bar{a}) - \frac{H}{R} q K_o'(\bar{a})} \tag{I-9}$$

and the solution of Equation (I-2) which satisfies Equations (I-3) and (I-4) is

$$\bar{U} = AK_o(\bar{r}) + C\left[I_o \int K_o \, d\bar{r} - K_o \int I_o \, d\bar{r} \right] \tag{I-10}$$

Because only a small time interval is of interest, the following asymptotic expansions of K_o and K_1, are used (Reference 4):

$$K_o(\bar{r}) = \left(\frac{\pi}{2\bar{r}}\right)^{\frac{1}{2}} e^{-\bar{r}} \left\{ 1 - \frac{1}{8\bar{r}} + \frac{9}{128\bar{r}^2} - \frac{75}{1024\bar{r}^3} + \cdots \right\} \tag{I-11}$$

$$K_1(\bar{r}) = \left(\frac{\pi}{2\bar{r}}\right)^{\frac{1}{2}} e^{-\bar{r}} \left\{ 1 + \frac{3}{8\bar{r}} - \frac{15}{128\bar{r}^2} + \frac{105}{1024\bar{r}^3} - \cdots \right\} \tag{I-12}$$

The resulting equation, after algebraic simplification, is

$$\begin{aligned} \bar{U}' = \left(\frac{1}{r'}\right)^{\frac{1}{2}} & \frac{e^{-q(r'-1)}}{p} \left\{ 1 - \left[\frac{r'-1}{8r'} - H \right] \frac{1}{q} + \right. \\ & + \left[H^2 + H\left(\frac{1}{8r'} - \frac{5}{8} - B \right) + \frac{9}{128r'^2} - \frac{1}{64r'} - \frac{7}{128} + \right. \\ & \left. \left. + B \right] \frac{1}{q^2} + \cdots \right\} - \frac{B}{Rr'p^2} - \frac{B}{R^2 r'^3 p^3} - \frac{9B}{R^3 r'^5 p^4} - \cdots \end{aligned} \tag{I-13}$$

* Similarly, expansions for I_o and I_1 can be obtained.

Using Standard transform tables (Reference 5) gives

$$U' = \frac{1}{\sqrt{\pi r'}}\left\{\operatorname{erfc}\left(\frac{r'-1}{\sqrt{\frac{4t'}{R}}}\right) + C_1\sqrt{\frac{4t'}{R}}\,\operatorname{ierfc}\left(\frac{r'-1}{\sqrt{\frac{4t'}{R}}}\right) + C_2\cdot\frac{4t'}{R}\,i^2\operatorname{erfc}\left(\frac{r'-1}{\sqrt{\frac{4t'}{R}}}\right) + \right.$$

$$\left. + C_3\left(\frac{4t'}{R}\right)^{\frac{3}{2}} i^3\operatorname{erfc}\left(\frac{r'-1}{\sqrt{\frac{4t'}{R}}}\right) + C_4\left(\frac{4t'}{R}\right)^2 i^4\operatorname{erfc}\left(\frac{r'-1}{\sqrt{\frac{4t'}{R}}}\right)\right\} - \qquad \text{(I-14)}$$

$$- B\left[\frac{t'}{Rr'} + \frac{t'^2}{2R^2r'^3} + \frac{9t'^3}{6R^3r'^5} + \frac{225t'^4}{24R^4r'^7} + \cdots\right]$$

The corresponding displacement, strain and strain-rate are

$$Z' = \frac{1}{\sqrt{\pi r'}}\left\{i^2\operatorname{erfc}\left(\frac{r'-1}{\sqrt{\frac{4t'}{R}}}\right) + C_1\sqrt{\frac{4t'}{R}}\,i^3\operatorname{erfc}\left(\frac{r'-1}{\sqrt{\frac{4t'}{R}}}\right) + C_2\cdot\frac{4t'}{R}\,i^4\operatorname{erfc}\left(\frac{r'-1}{\sqrt{\frac{4t'}{R}}}\right) + \right.$$

$$\left. + C_3\left(\frac{4t'}{R}\right)^{\frac{3}{2}} i^6\operatorname{erfc}\left(\frac{r'-1}{\sqrt{\frac{4t'}{R}}}\right)\right\} - \qquad \text{(I-15)}$$

$$- B\left[\frac{t'}{8Rr'} + \frac{t'^2}{24R^2r'^3} + \frac{9t'^3}{96R^3r'^5} + \frac{225t'^4}{480R^4r'^7} + \cdots\right]$$

$$\frac{\partial U'}{\partial r'} = -\frac{1}{\sqrt{\pi r'}}\left\{\frac{2}{\sqrt{\pi}}\cdot\frac{1}{\sqrt{\frac{4t'}{R}}}\,e^{\frac{-(r'-1)^2R}{4t'}} + C_5\operatorname{erfc}\left(\frac{r'-1}{\sqrt{\frac{4t'}{R}}}\right) + C_6\sqrt{\frac{4t'}{R}}\,\operatorname{ierfc}\left(\frac{r'-1}{\sqrt{\frac{4t'}{R}}}\right) + \right.$$

$$\left. + C_7\cdot\frac{4t'}{R}\,i^2\operatorname{erfc}\left(\frac{r'-1}{\sqrt{\frac{4t'}{R}}}\right) + C_8\left(\frac{4t'}{R}\right)^{\frac{3}{2}} i^3\operatorname{erfc}\left(\frac{r'-1}{\sqrt{\frac{4t'}{R}}}\right)\right\} + \qquad \text{(I-16)}$$

$$+ B\left[\frac{t'}{Rr'^2} + \frac{3t'^2}{2R^2r'^4} + \frac{45t'^3}{6R^3r'^6} + \frac{1575t'^4}{24R^4r'^8} + \cdots\right]$$

$$\frac{\partial z}{\partial r'} = -4t' \cdot \frac{1}{\sqrt{r'}} \left\{ \frac{1}{\sqrt{\frac{4t'}{R}}} \, \text{ierfc}\left(\frac{r'-1}{\sqrt{\frac{4t'}{R}}}\right) + C5 \cdot i^2\text{erfc}\left(\frac{r'-1}{\sqrt{\frac{4t'}{R}}}\right) + C6 \sqrt{\frac{4t'}{R}} \cdot i^3\text{erfc}\left(\frac{r'-1}{\sqrt{\frac{4t'}{R}}}\right) + \right.$$

$$\left. + C7 \cdot \frac{4t'}{R} \cdot i^4\text{erfc}\left(\frac{r'-1}{\sqrt{\frac{4t'}{R}}}\right) \right\} + B\left[\frac{t'}{8Rr'^2} + \frac{t'^2}{8R^2r'^4} + \frac{45t'^3}{96R^3r'^6} + \frac{1575t'^4}{480R^4r'^8} + \cdots \right] \qquad \text{(I-17)}$$

where,

$$C1 = \left(\frac{1}{8} - H\right) - \frac{1}{8r'}$$

$$C2 = \left(H^2 - \frac{5}{8}H - BH - \frac{7}{128} + B\right) + \left(\frac{H}{8} - \frac{1}{64}\right)\frac{1}{r'} + \frac{9}{128r'^2}$$

$$C3 = \left(-H^3 + \frac{9}{8}H^2 + BH^2 + \frac{15}{128}H - \frac{9}{8}BH + \frac{B}{8} + \frac{59}{1024}\right) + \left(-\frac{H^2}{8} + \frac{5}{64}H + \frac{B}{8}H + \frac{7}{1024} - \right.$$

$$\left. - \frac{B}{8}\right)\frac{1}{r'} + \left(-\frac{9}{128}H + \frac{9}{1024}\right)\frac{1}{r'^2} - \frac{75}{1024r'^3}$$

$$C4 = \left(H^4 - \frac{13}{8}H^3 - BH^3 + \frac{9}{128}H^2 + \frac{13}{8}BH^2 - \frac{143}{1024}H + \frac{55}{128}BH + \frac{121}{128}B - \frac{3013}{32768}\right) +$$

$$+ \left(\frac{H^3}{8} - \frac{9}{64}H^2 - \frac{1}{8}BH^2 - \frac{15}{1024}H + \frac{9}{64}BH - \frac{B}{64} - \frac{59}{8192}\right)\frac{1}{r'} +$$

$$+ \left(\frac{9}{128}H^2 - \frac{45}{1024}H - \frac{9}{128}BH + \frac{9}{128}B - \frac{63}{16384}\right)\frac{1}{r'^2} +$$

$$+ \left(\frac{75}{1024}H - \frac{75}{8192}\right)\frac{1}{r'^3} + \frac{3675}{32,768r'^4}$$

$$C_5 = \left(\frac{1}{8} - H\right) + \frac{3}{8r_1}$$

$$C_6 = \left(H^2 - \frac{5}{8}H - B_{1,1} - \frac{7}{128} + B\right) + \left(-\frac{3}{8}H + \frac{3}{64}\right)\frac{1}{r_1} - \frac{15}{128r_{1,2}}$$

$$C_7 = \left(-H^3 + \frac{9}{8}H^2 + BH^2 + \frac{15}{128}H - \frac{9}{8}BH + \frac{B}{8} + \frac{59}{1024}\right) + \left(\frac{3}{8}H^2 - \frac{15}{64}H -\right.$$

$$\left. - \frac{3}{8}BH + \frac{3}{8}B - \frac{21}{1024}\right)\frac{1}{r_1} + \left(\frac{15}{128}H - \frac{15}{1024}\right)\frac{1}{r_{1,2}} + \frac{105}{1024r_{1,3}}$$

$$C_8 = \left(H^4 - \frac{13}{8}H^3 - BH^3 + \frac{9}{128}H^2 + \frac{13}{8}BH^2 - \frac{143}{1024}H + \frac{55}{128}BH + \frac{121}{128}B - \frac{3013}{32,768}\right) +$$

$$+ \left(-\frac{3}{8}H^3 + \frac{27}{64}H^2 + \frac{3}{8}BH^2 + \frac{45}{1024}H - \frac{27}{64}BH + \frac{3}{64}B + \frac{177}{8192}\right)\frac{1}{r_1} +$$

$$+ \left(-\frac{15}{128}H^2 + \frac{75}{1024}H + \frac{15}{128}BH - \frac{15}{128}B + \frac{105}{16,384}\right)\frac{1}{r_{1,2}} +$$

$$+ \left(-\frac{105}{1024}H + \frac{105}{8192}\right)\frac{1}{r_{1,3}} - \frac{4725}{32,768r_{1,4}}$$